

Original Article

NUDCD1 promotes metastasis through inducing EMT and inhibiting apoptosis in colorectal cancer

Bin Han^{1,2*}, Yuan-Yuan Zhang^{1*}, Ke Xu¹, Yang Bai¹, Li-Hong Wan¹, Shi-Kun Miao¹, Ke-Xian Zhang³, Hong-Wei Zhang³, Yin Liu^{1,3}, Li-Ming Zhou¹

¹Department of Pharmacology, West China School of Preclinical and Forensic Medicine, Sichuan University, Chengdu 610041, Sichuan Province, China; ²Department of Pharmacy, Affiliated Hospital of North Sichuan Medical College, Nanchong 637000, Sichuan Province, China; ³Department of Anesthesiology, Sichuan Cancer Hospital & Institute, Sichuan Cancer Center, University of Electronic Science and Technology of China, Chengdu 610041, Sichuan Province, China. *Equal contributors.

Received February 20, 2018; Accepted April 16, 2018; Epub May 1, 2018; Published May 15, 2018

Abstract: Colorectal cancer (CRC) is the third most commonly diagnosed cancer and the third leading cause of cancer death in both men and women. NudC domain containing 1 (NUDCD1) was identified as an oncoprotein which was activated or over-expressed in various human cancers. We aimed to investigate the effects and mechanisms of NUDCD1 in human CRC. The expression of NUDCD1 in CRC and pericarcinous tissues from 70 CRC patients were determined by real-time PCR, western blotting, and immunohistochemistry. The correlation between the expression of NUDCD1 and clinical characteristics was analyzed. The expression of NUDCD1 in five CRC cell lines and normal colon mucosal epithelial cell line was measured by real-time PCR. Then we knock down NUDCD1 in HCT116 and HT 29 cells. The cell viability assay, scratch assay, migration and invasion assay and flow cytometry were used to analyze NUDCD1's effects on the proliferation, migration, invasion, cell cycle and apoptosis of CRC cells. NUDCD1's effects on CRC xenografts of nude mice was also determined. Results showed that the expression of NUDCD1 was much higher in CRC tissues than that in pericarcinous tissues. Over-expression of NUDCD1 in human CRC tissues was significantly associated with lymph node metastasis, distant metastasis, and advanced stages. The expression of NUDCD1 was higher in all of the CRC cell lines than that in normal colon epithelial mucosal cells. To knockdown NUDCD1 resulted in significant decreases in cell viability and proliferation, decreased protein expression of N-cadherin and increased protein expression of E-cadherin which were biomarkers of EMT, arrested the cell cycle and increased apoptosis via down-regulated cyclin D1, Bcl2, and up-regulated cleaved-caspase3. Furthermore, to knockdown NUDCD1 inactivated IGF1R-ERK1/2 signaling pathway in vitro and in vivo, and suppressed the xenografts of CRC. In conclusion, NUDCD1 promotes the carcinogenesis and metastasis of CRC through inducing EMT and inhibiting apoptosis, which suggests NUDCD1 be a potential biomarker for CRC.

Keywords: Colorectal cancer, NUDCD1, EMT, apoptosis

Introduction

Colorectal cancer (CRC), highly resistant to chemotherapy, growing rapidly with early vascular and lymph invasion, is the second leading cause of cancer-related deaths in developed countries [1]. Largely due to the distant metastasis and high frequency of tumor recurrence, CRC patients were associated with an extremely poor prognosis after surgical resection [2, 3]. Recent statistics showed that the incidence rate of CRC had been dramatically increasing with years in China, ranking only after lung cancer and gastric cancer [4]. Although multiple

genes in the process of tumor recurrence and metastasis have been identified, the underlying mechanism of CRC metastasis remains unclear [5-7]. Looking for reliable biomarkers for recurrence and metastasis will greatly benefit CRC patients and may provide novel gene targets for CRC treatment.

NudC domain containing 1 (also known as NUDCD1, CML66, or OVA66), identified as an oncoprotein frequently activated or over-expressed in various human cancers, was known as an important kind of protein named cancer antigen [8, 9]. It was also involved in regulating

Molecular mechanisms of colorectal cancer

Table 1. Relationship between NUDCD1 levels in CRC tissues and clinical pathological features (n=70)

Clinical characteristics	N (%)	NUDCD1 relative expression		Mean ± SEM	P
		Up-regulation (%)	Down-regulation (%)		
Age					
>60	32 (45.7)	22 (31.4)	10 (14.3)	3.56 ± 0.64	0.328
≤60	38 (54.3)	27 (38.6)	11 (15.7)	2.79 ± 0.45	
Sex					
Male	37 (52.9)	24 (34.3)	13 (18.6)	2.75 ± 0.45	0.224
Female	33 (47.1)	25 (35.7)	8 (11.4)	3.34 ± 0.58	
T Division					
T1-T2	7 (10.0)	3 (4.3)	4 (5.7)	2.07 ± 1.29	0.610
T3-T4	63 (90.0)	42 (60.0)	21 (30.0)	2.79 ± 0.37	
Lymph Invasion					
N0	34 (48.6)	18 (25.7)	16 (22.9)	2.13 ± 0.42	0.041
N1-N2	36 (51.4)	30 (42.9)	6 (8.6)	3.36 ± 0.55	
Metastasis					
M0	60 (85.7)	39 (55.7)	21 (30.0)	2.69 ± 0.36	0.003
M1	10 (14.3)	10 (14.3)	0 (0.0)	5.83 ± 1.20	
Duke Division					
I-II	33 (47.1)	18 (25.7)	15 (21.4)	2.30 ± 0.44	0.031
III-IV	37 (52.9)	31 (44.3)	6 (8.6)	3.90 ± 0.57	

different biological processes, such as apoptosis and immune responses. It was reported that over-expression of NUDCD1 enhanced the proliferation, invasion, and survival of HO-8910 cells via regulating IGF-1R-MAPK signaling pathway [10]. Over-expression of NUDCD1 can confer tumorigenicity to NIH3T3 cells, and inhibit the apoptosis of cultured human tumor cells which exposed to chemotherapeutic agents via hyper-activating PI3K-AKT and ERK1/2-MAPK signaling pathway [11]. Although current evidence suggested that NUDCD1 may act as an oncoprotein, its expression and molecular mechanisms in CRC metastasis remain unclear.

Therefore we hypothesized that NUDCD1 over-expression plays a metastatic role during the progression of colorectal mucosa to CRC. To test our hypothesis, we extensively measured NUDCD1 expression in human CRC tissues and determined its contribution to CRC proliferation, invasion, and metastasis in vitro and in vivo. We also investigated the molecular mechanisms by which NUDCD1 mediates metastasis. Our results demonstrated that NUDCD1 was over-expressed in CRC tissues and cells, playing a major metastatic role in growth, epithelial-mesenchymal transition (EMT) and

apoptosis of CRC cells via regulating IGF1R-ERK1/2 signaling pathway.

Materials and methods

Patients and samples

To determine the expression of NUDCD1 in CRC tissues, 70 cases of CRC patients who underwent radical surgery in the Department of General Surgery, West China Hospital, Sichuan University, from May 2010 to Sep 2011 were included in the study. The CRC and pericarcinous tissues (negative control, NC) were surgically resected. A part of each sample was

quickly stored in liquid nitrogen for real-time PCR and western blotting. Part of each sample for immunohistochemistry detection was fixed by 4% paraformaldehyde (Boster, Wuhan, China) for 24 hours, then dehydrated and embedded in paraffin. The pericarcinous tissues which were away from tumors at least 5 cm, did not contain cancer cells. General information of these patients was summarized in **Table 1**. The CRC tissues were further divided into well (WD) or poorly differentiated (PD) groups by two pathologists independently. All tissue samples were collected from consenting individuals according to the protocols approved by the Ethics Review Board of Sichuan University.

Cell culture

All of the cell lines in this study were kept in the Department of Pharmacology, West China School of Preclinical and Forensic Medicine, Sichuan University. The normal colon mucosal epithelial cell line, NCM460, was purchased from the Type Culture Collection of the Chinese Academy of Sciences (Shanghai, China). Five CRC cell lines, SW620, HCT116, HT29, SW480 and DLD1 cells, were purchased from American Type Culture Collection (ATCC; Manas-

sas, VA, USA). The cells were cultured with Dulbecco's modified eagle medium (DMEM) high glucose medium (HyClone, Logan, UT, USA) supplemented with 10% fetal bovine serum (Shengong, Shanghai, China) and 1% penicillin-streptomycin solution (HyClone, Logan, UT, USA) at 37°C in 5% CO₂.

Real-time PCR

Total RNA (1 µg) was obtained by E.Z.N.A.[®] Total DNA/RNA/Protein Kit (Omega Bio-Tekinc, Norcross, GA), and subjected to reverse transcription with a Revert Aid First Strand cDNA Synthesis Kit (Thermo scientific Inc, MA, USA) according to the manufacturer's protocol. Quantitative real-time polymerase chain reaction (real-time PCR) was performed with SYBR[®] Premix Ex TaqTMII (Tli RnaseH Plus) (Takara Bio Inc, Japan) and CFX96TM Real-Time PCR Detection System. The primers were as follows: NUDCD1-forward: 5'-CTGTGGCAGAGGT-AAAACCTTC-3'; NUDCD1-reverse: 5'-GACAAGG-TAACCCAGGTAGAAG-3'; GAPDH-forward: 5'-AG-AAGGCTGGGGCTCATTTC-3'; GAPDH-reverse: 5'-ACAGTCTTCTGGGTGGCAGTG-3'.

The relative expression of NUDCD1 was analyzed with the 2^{-ΔΔCt} method [12].

Immunohistochemistry (IHC) detection

All of the paraffin-embedded specimens were sectioned into 5 µm slides. The sections were incubated with rabbit polyclonal antibody against NUDCD1 (Abcam, Cambridge, UK), then incubated with immunohistochemical assay kit (Boster, Wuhan, China) according to manufacturer's instructions, subsequently stained with DAB (Beyotime, Shanghai, China) and hematoxylin (Beyotime, Shanghai, China) [10]. Protein expressions of NUDCD1 were visualized by the optical microscope (TS100-F, Nikon, Japan). All of the slices were observed under the optical microscope (Olympus, Japan), 5 fields of each slice were randomly captured. The average optical density (IOD/Area) of the pictures was measured by Imagepro-plus 6.0 (Media Cybernetics, PA, USA) for the semi-quantitative analysis of the expression of NUDCD1.

Western blot analysis

The total protein was extracted by E.Z.N.A.[®] Total DNA/RNA/Protein Kit (Omega Bio-Tekinc, Norcross, GA). Protein concentrations were

determined by the BCA protein assay kit (Pierce Biotechnology, Rockford, IL). Equal amounts of proteins were mixed with loading buffer, boiled for 5 min, and separated on 10% SDS-PAGE. Protein samples (50 µg) were subjected to 10% sodium dodecyl sulfate-polyacrylamide gel electrophoresis (SDS-PAGE), and then electronically transferred to polyvinylidene fluoride (PVDF) membrane (Millipore, USA). The blot was blocked with 5% non-fat milk at room temperature for 1 h and then incubated with primary antibody at 4°C overnight. The membrane was then incubated with goat anti-rabbit secondary antibody (Abcam, Cambridge, UK) at room temperature for 1 h. Electro-Chemi-Luminescence (ECL) detect kit (Beyotime, Shanghai, China) was used for blot chemi-luminescence. Image lab 3.0 software (Bio-Rad, GA, USA) was used to obtain and analyze the signal. The target proteins were normalized against the loading control GAPDH.

Plasmids construction and transfection

Based on the available information at CRISPR Design (<http://crispr.mit.edu>), clustered regularly interspaced short palindromic repeats (CRISPRs) for NUDCD1 were designed according to the Zhang laboratory's protocol [13] and then cloned into the lentiCRISPR/CAS9 vector by the following pHBCas9n (D10A)/gRNA Easy KO Reagent (Hanbio, Shanghai, China) manufacturer's protocols.

The sgRNA sequence targeted 5'-GGCGGCT-AATTGCTCCCTAC-3'. The primer sequences of NUDCD1 CRISPR were: 5'-CACCGCGCGCTAATTGCTCCCTAC-3'; 5'-AAACGTAGGGAGCAATTAG-CCGCC-3'. The primer sequences of negative control CRISPR were: 5'-CACCGTCTGTGTCTGGGCCATTTT-3'; 5'-AAACAAAATGGCCCAGACACAGAAC-3'.

For NUDCD1 over-expression, the gene sequences encoding NUDCD1 was amplified from HCT-116 cells using ClonExpress II One Step Cloning Kit (Vazyme, Nanjing, China) and cloned into the pcDNA3.1 plasmid according to the manufacturer's instructions.

When growing to 50%-70% confluence, cells were transfected with plasmids (2 µg/mL in complete growth media) by using ExFect Transfection Reagent (Vazyme, Nanjing, China) according to the manufacturer's instructions.

Molecular mechanisms of colorectal cancer

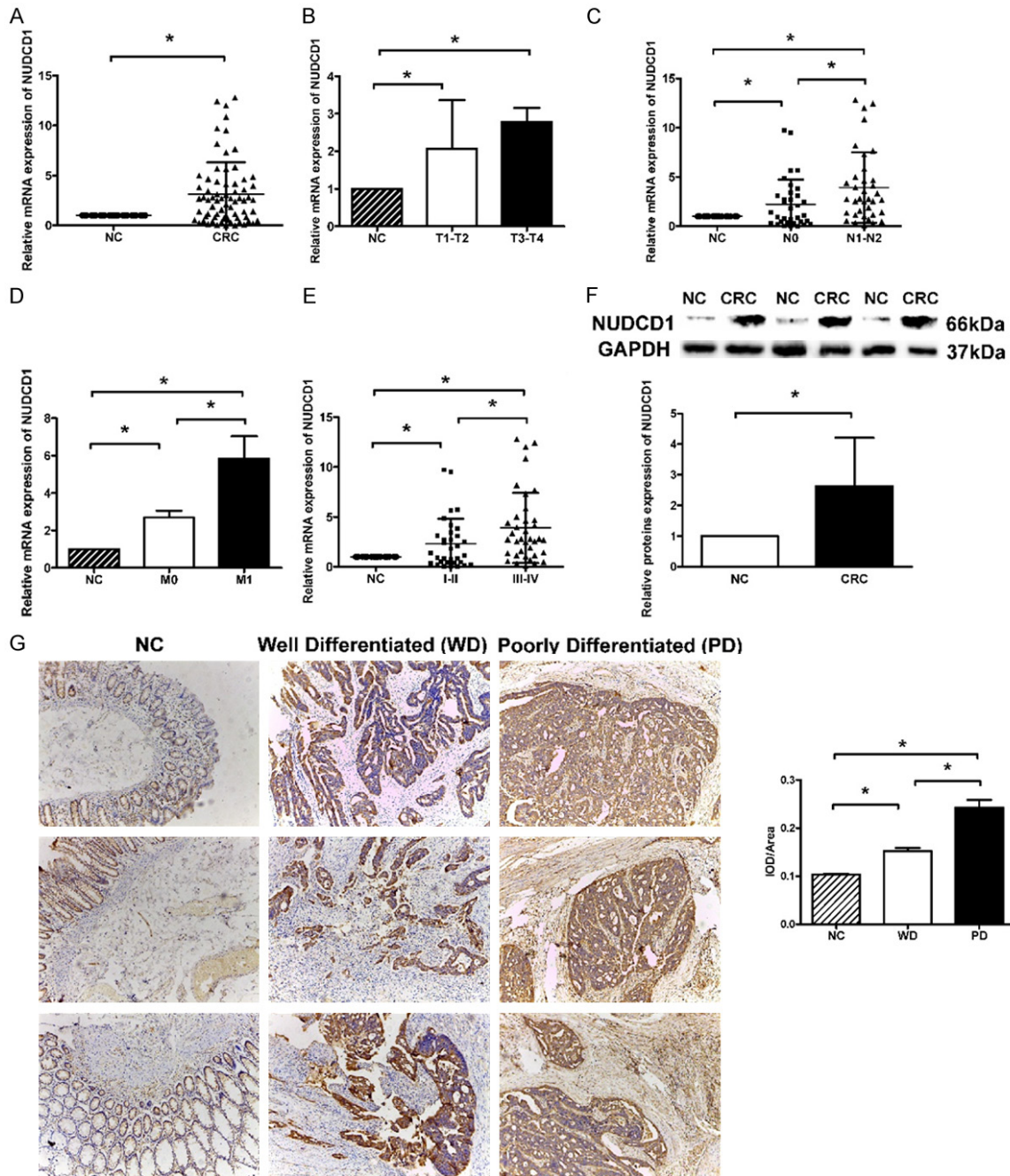


Figure 1. The expression of NUDCD1 was significantly increased in human CRC tissues (CRC) than that in pericarcinous tissues (NC). Relative NUDCD1 mRNA expression in human CRC tissues and cell lines was detected by real-time PCR. A. Relative NUDCD1 expression in CRC tissues and adjacent pericarcinous tissues. B. Relative NUDCD1 expression in CRC tissues with T1-T2, T3-T4 stages, and adjacent pericarcinous tissues. C. Relative NUDCD1 expression in CRC tissues from patients with lymph metastasis (N1-N2), without lymph metastasis (N0) and adjacent pericarcinous tissues. D. Relative NUDCD1 expression in CRC tissues from patients with metastasis (M1), without metastasis (M0) and adjacent pericarcinous tissues. E. Relative NUDCD1 expression in CRC tissues from patients with duke stage I-II, III-IV, and adjacent pericarcinous tissues. F. Relative NUDCD1 protein expression in human CRC tissues and adjacent pericarcinous tissues. G. Immunohistochemistry staining of CRC tissues and adjacent pericarcinous tissues (100×). Results display the mean \pm SEM from triplicate experiments, * $P < 0.05$.

Cell Proliferation (MTS) assay

To determine the effects of NUDCD1 on the proliferation of CRC cells, HCT116 and HT29

cells were transfected with plasmid NC-sgRNA or NUDCD1-sgRNA and maintained in DMEM high glucose medium (HyClone, Logan, UT, USA) supplemented with 10% FBS at 37°C in

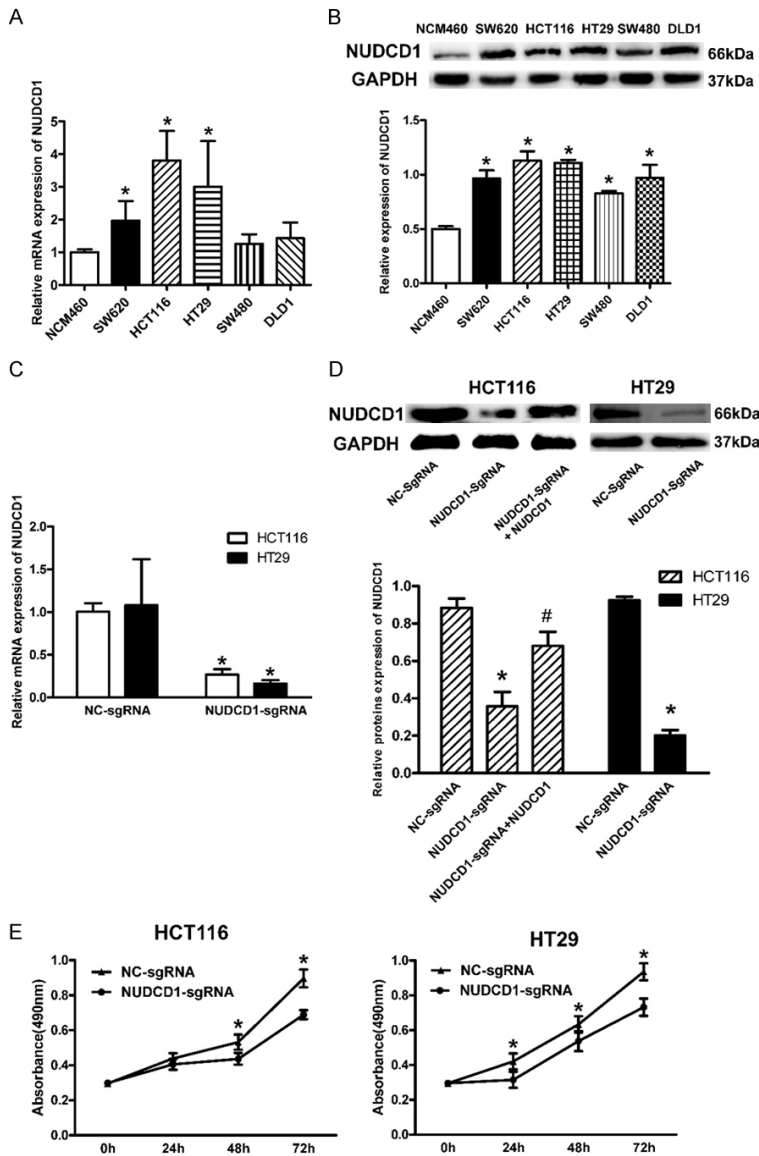


Figure 2. The expression of NUDCD1 in different CRC cell lines and its effect on the proliferation of CRC cells. A. Relative NUDCD1 expression in the normal colon mucosal epithelial cell line, NCM460, and five CRC cell lines, SW620, HCT116, HT29, SW480, and DLD1. B. Relative NUDCD1 protein expression in NCM460 cells and SW620, HCT116, HT29, SW480 and DLD1 cells. Then HCT116 and HT29 were transfected with NUDCD1-sgRNA or NC-sgRNA, respectively. C. Relative NUDCD1 mRNA expression in HCT116 and HT29 cells after transfection. D. Relative NUDCD1 protein expression in HCT116 and HT29 cells after transfection. E. Cell viability of HCT116 and HT29 cells was measured by MTS assay. Cell growth curves were plotted according to the absorbance at 490 nm. Results display the mean \pm SEM from triplicate experiments. * $P < 0.05$, compared with NCM460 or NC-sgRNA, # $P < 0.05$, compared with NUDCD1-sgRNA.

5% CO₂. Cytotoxicity test was performed using the CellTiter 96 Aqueous One Solution Cell Proliferation Assay (MTS) reagent (Promega, WI, USA) to determine the number of viable cells following the manufacturer's instructions.

fields were randomly selected, and their images were obtained under the microscope (100 \times). The number of transmembrane cells was calculated, then the migration and invasion were evaluated.

After incubation of 0, 24, 48, 72 h, the cells were harvested for analysis. The optical density was measured at 490 nm using a spectrophotometer (Bio-Rad, USA).

Wound healing assay

To determine the effects of NUDCD1 on the migration of CRC cells wound healing assay was performed as previously described [14]. HCT116 and HT29 cells were cultured in a 24-well plate and transfected with NUDCD1-sgRNA or NC-sgRNA for 48 h. The cell monolayer in each well was scraped with a p200 pipet tip to create a gap. After washing with culture medium to remove cell debris, the cells were allowed to migrate for 24 hours, then observed under an optical microscope. The relative migration was calculated by the ratio of the distance after experiment to the distance before experiment.

Cell migration and invasion assay

48 h after transfection, the migration and invasion of the HCT116 and HT29 cells transfected with NUDCD1-sgRNA or NC-sgRNA were analyzed by using QCM Laminin Migration Assay kit (ECM220, Merck Millipore, Darmstadt, Germany) and Cell Invasion Assay kit (ECM 550, Merck Millipore, Darmstadt, Germany). Cells on the below surface of the membrane were stained according to the manufacturer's protocols. Eventually, cells were counted as follows: five

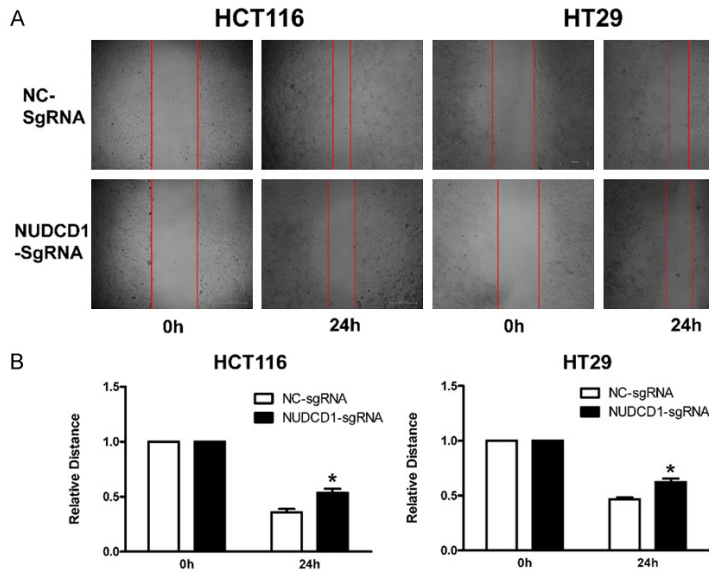


Figure 3. To knockdown NUDCD1 inhibited the migration of HCT116 and HT29 cells. A. Wound healing assay was used to assess the migration of HCT116 and HT29 cells transfected with NUDCD1-sgRNA or NC-sgRNA, respectively. B. Quantification of migration distance of HCT116 and HT29 cells. Results display the mean \pm SEM from triplicate experiments. *P < 0.05, compared with NC-sgRNA.

Cell cycle and apoptosis assay

48 h after transfection, the HCT116 and HT29 cells transfected with NUDCD1-sgRNA or NC-sgRNA were fixed with 75% ethanol at 4°C overnight, incubated with 1 mg/mL RNaseA for 30 min at 37°C, and stained with propidium iodide (PI; Beyotime, Shanghai, China) according to the manufacturer’s instructions. Subsequently, the stained cells were analyzed by flow cytometry.

Also 48 h after transfection, for cell apoptosis analysis, the transfected cells were washed with PBS and re-suspended in the binding buffer. 100 μ L cell suspension was added with 5 μ L Annexin V-FITC (Vazyme, Nanjing, China) and 5 μ L PI (Vazyme, Nanjing, China), then incubated for 15 min in the darkness. After the incubation, 400 μ L binding buffer was added into the suspension for flow cytometry assay. The apoptosis was analyzed by CFlow plus 1.0 software (BD Biosciences, NJ, USA). On the other hand, for the observation of cell apoptosis, cells were washed with PBS and stained with PI for 15 min in the darkness. Subsequently, the cells were stained with Hoechst 33342 (Beyotime, Shanghai, China) for 15 min. Eventually, the stained cells were observed by fluorescence microscope.

Animal studies

Twelve male BALB/c-nu mice (4-5 weeks of age, 18-22 g) were purchased from Das-huo experimental animal company, Sichuan, China. Mice were maintained under specific pathogen-free conditions, 12 hours light/dark cycle with free access to water and food. All experimental procedures were approved by the Ethics Review Board of Sichuan University. 1×10^6 HCT116 cells were subcutaneously injected into the flank of each mouse. The nude mice were divided into two groups: six mice (negative control group) were transfected with NC-sgRNA plasmid (10 μ g each mouse) in vivo via xenograft injection every 4 days, and the others were transfected with

NUDCD1-sgRNA plasmid in the same way. The transfections were conducted with Entranster in vivo (Engreen Biosystem, Beijing, China) according to the manufacturer’s instructions and the protocols provided in literatures [15, 16]. Four weeks later, all mice were sacrificed. Xenografts were dissected and weighed, then quickly stored in liquid nitrogen for real-time PCR and western blotting.

Statistical analysis

SPSS software (version 20.0, SPSS, Inc., Chicago, IL, USA) was used for statistical analysis. All the experiments were repeated three times. Data were expressed as the mean \pm standard error of mean (SEM). The continuous variables were compared using an unpaired Student t test or a Mann-Whitney U test if the variables were not normally distributed. P < 0.05 was considered to indicate a statistically significant difference.

Results

The relative mRNA and protein expression of NUDCD1 in CRC tissues and cell lines

The general information of 70 CRC patients was summarized in **Table 1**. Expression of

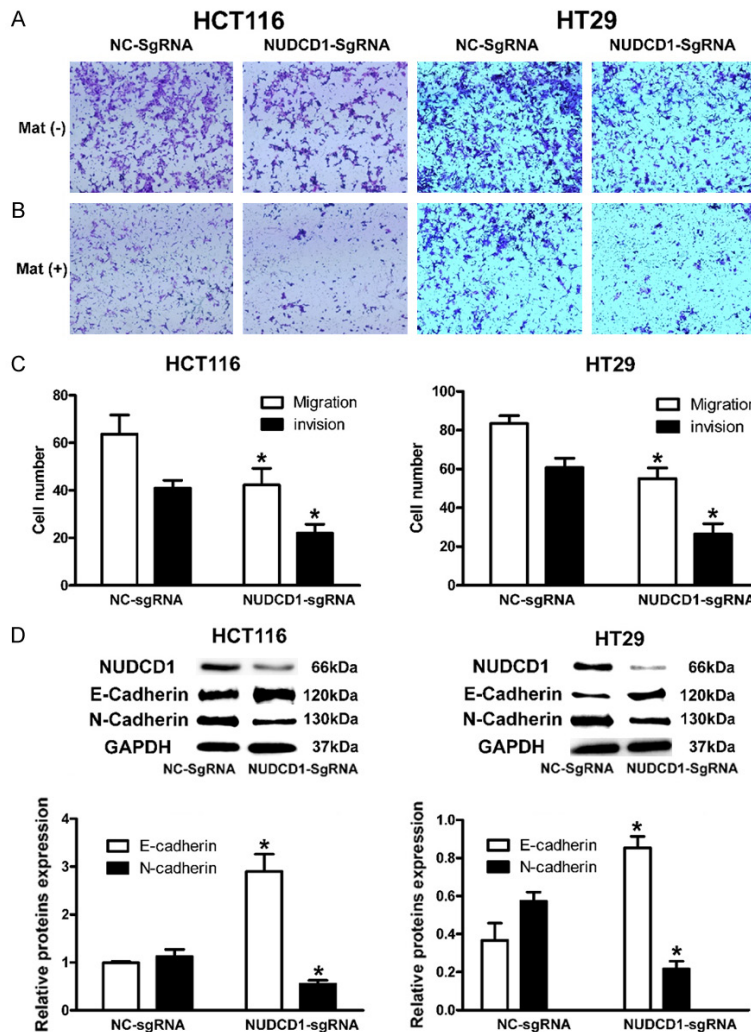


Figure 4. To knockdown NUDCD1 inhibited the migration and invasion of HCT116 and HT29 cells. Transwell migration (A) and invasion assay (B) were conducted with HCT116 and HT29 cells transfected with NUDCD1-sgRNA or NC-sgRNA, respectively (100×). (C) Quantification of cell numbers of the transwell migration and invasion assays. (D) Relative protein expression of the biomarkers of EMT, E-cadherin and N-cadherin, by western blotting. Results display the mean ± SEM from triplicate experiments. *P < 0.05, compared with NC-sgRNA.

NUDCD1 mRNA was significantly up-regulated in CRC tissues compared to the pericarcinoma tissues (Figure 1A). As shown in Figure 1B-E, the correlation between NUDCD1 and clinical characteristic of CRC patients was analyzed. Up-regulation of NUDCD1 protein was also observed in these clinical specimens (Figure 1F), and NUDCD1 protein was located in the cytoplasm and on the membrane (Figure 1G). In addition, real-time PCR and western blotting were used to measure the mRNA and protein expression of NUDCD1 in normal colon mucosal epithelial cell line NCM460 and five human CRC cell lines, SW620, HCT116, HT29, SW480,

and DLD1 cells. As shown in Figure 2A and 2B, all of the five CRC cell lines displayed higher mRNA and protein expression of NUDCD1 than that of NCM460 cells. Our results showed that overexpression of NUDCD1 in CRC tissues was significantly correlated with lymph node metastasis, distant metastasis, and advanced CRC stages, which indicated that NUDCD1 might promote the carcinogenesis and metastasis of CRC.

To knockdown NUDCD1 inhibited the proliferation of CRC cells

To determine the effects of NUDCD1 on the proliferation of CRC cells, CRISPR/Cas9 plasmid of NUDCD1 (NUDCD1-sgRNA) and its negative control (NC-sgRNA) were designed and chemically synthesized. Since NUDCD1 was most highly expressed in HCT116 and HT29 cells, these two cell lines were chosen to be transfected with these plasmids in vitro, respectively. Compared with the negative control, the mRNA and protein expression of NUDCD1 were significantly down-regulated in HCT116 and HT29 cells transfected with NUDCD1-sgRNA (Figure 2C and 2D). Recovered NUDCD1 were observed in HCT116 cells after

co-transfection with NUDCD1-sgRNA and NUDCD1 overexpression plasmids (Figure 2D). As shown in the results of MTS assay, to knockdown NUDCD1 can obviously inhibit the proliferation of HCT116 and HT29 cells (Figure 2E).

To knockdown NUDCD1 suppressed the migration and invasion of CRC cells through inhibiting EMT

To determine the effects of NUDCD1 on the migration and invasion of CRC cells, we performed wound-healing and transwell assays (with matrix-gel or not). As shown in Figures 3,

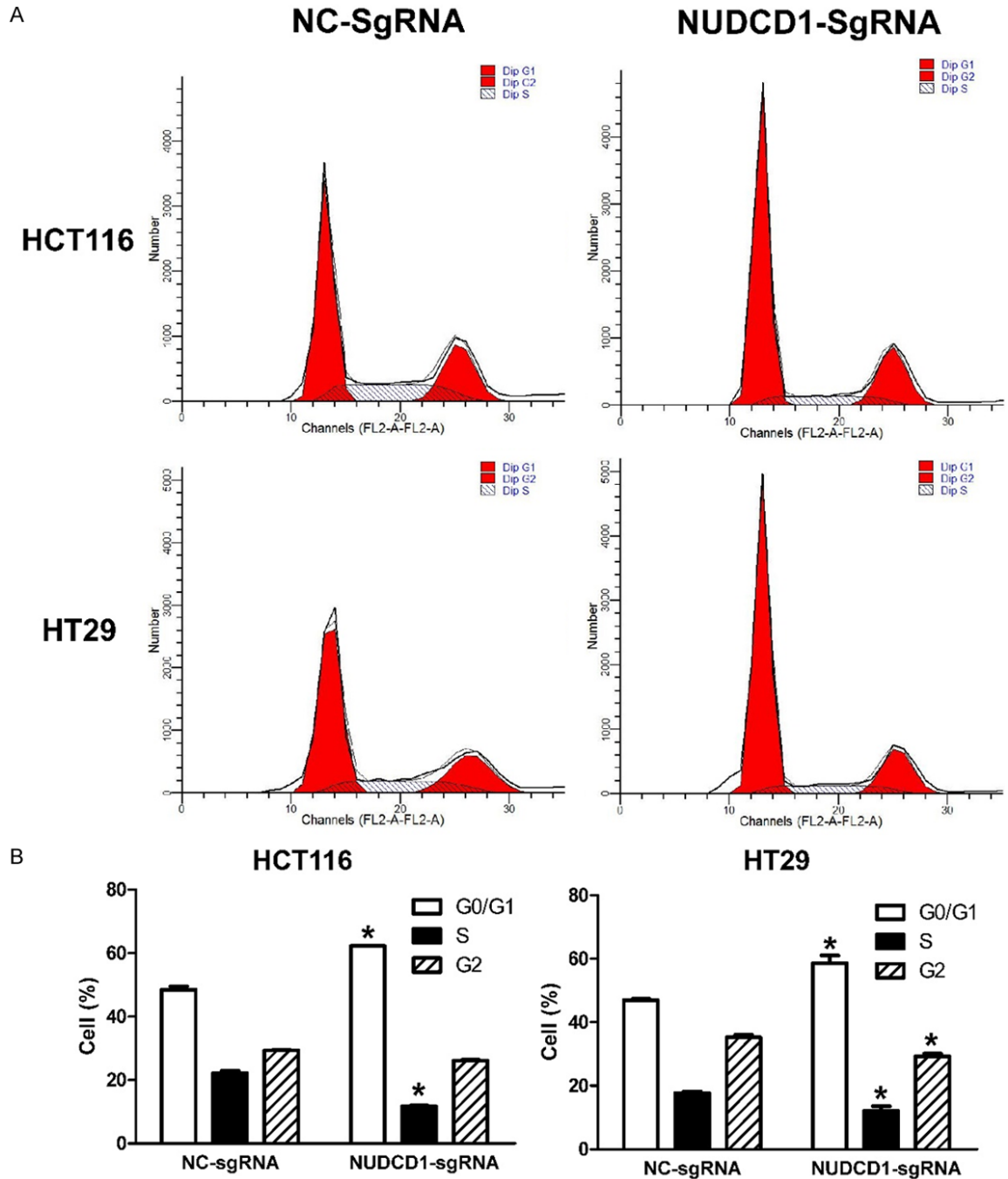


Figure 5. To knockdown NUDCD1 resulted in the cell cycle arrest of HCT116 and HT29 cells. A. Cells were stained with PI and DNA content was detected by flow cytometry at 72 h after transfection. B. Percentage of cells from A. Results display the mean \pm SEM from triplicate experiments. * $P < 0.05$, compared with NC-sgRNA.

4A and 4C, to knockdown NUDCD1 significantly inhibited the migration of HCT116 and HT29 cells. Results of transwell assays with matrix-gel demonstrated that to knockdown NUDCD1 inhibited the invasion of HCT116 and HT29 cells (Figure 4B and 4C). To determine the effects of NUDCD1 on EMT, we determined the expression of two important biomarkers of

EMT, N-cadherin, and E-cadherin, by western blotting. Our results demonstrated that to knockdown NUDCD1 decreased the expression of N-cadherin, and increased the expression of E-cadherin in HCT116 and HT29 cells (Figure 4D), which indicated that NUDCD1 suppressed the migration and invasion of CRC cells through inhibiting EMT.

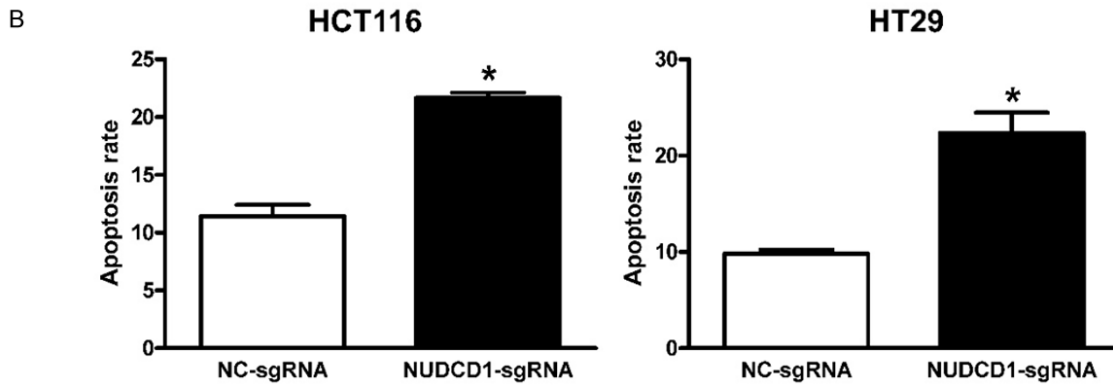
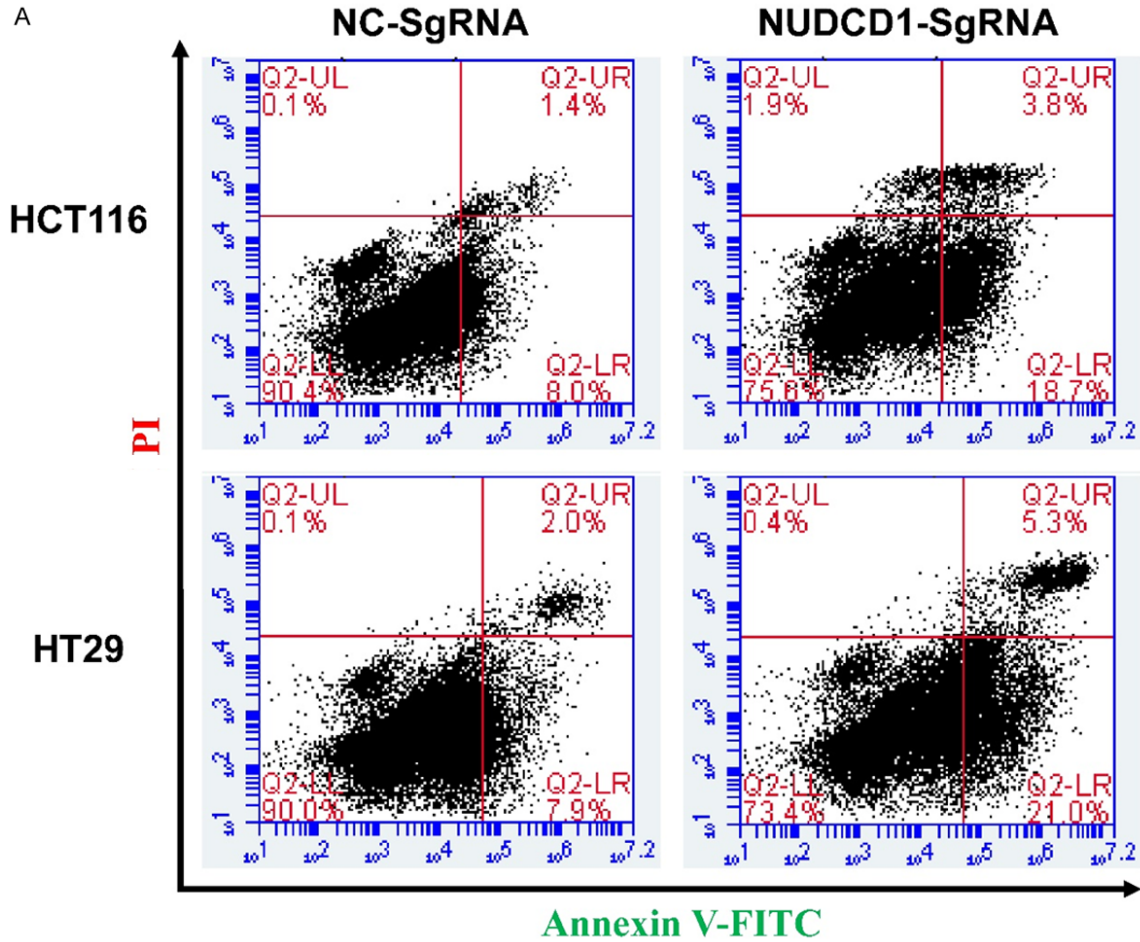


Figure 6. To knockdown NUDCD1 promoted the apoptosis of HCT116 and HT29 cells. A. Cells were stained with Annexin V-FITC and PI at 72 h after transfection. The ratio of apoptosis was detected by flow cytometry. Q2: detected cells; LL: viable cells, LR: early apoptotic cells; UR: late apoptotic cells; UL: necrotic cells. B. Quantification of percentage of apoptotic cells from A. Results display the mean \pm SEM from triplicate experiments. *P < 0.05, compared with NC-sgRNA.

To knockdown NUDCD1 induced the cell cycle arrest and apoptosis of CRC cells

To investigate the effects of NUDCD1 on the cell cycle and apoptosis of CRC cells, HCT116 and HT29 cells were transfected with NUDCD1-

sgRNA or NC-sgRNA, respectively. Then they were stained with PI, Annexin V-FITC/PI and Hoechst 33342/PI, respectively, then analyzed by flow cytometer and observed by fluorescence microscope. As shown in **Figure 5**, to knockdown NUDCD1 increased the proportion

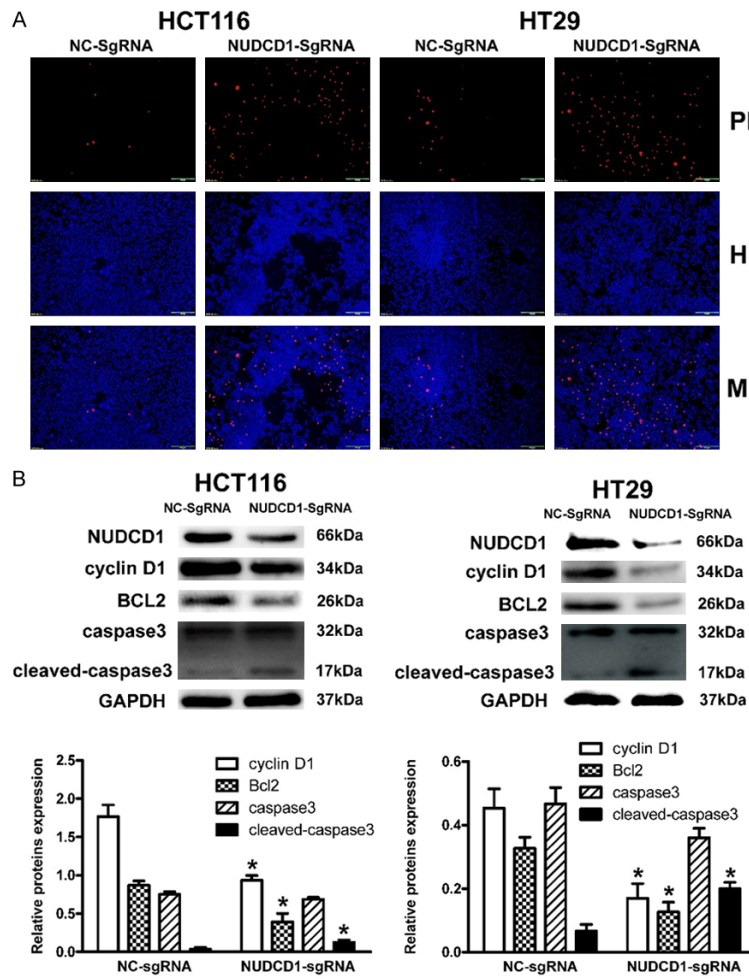


Figure 7. To knockdown NUDCD1 resulted in the apoptosis of HCT116 and HT29 cells. A. HCT116 and HT29 cells were stained with Hoechst 33342 and PI. The apoptotic cells were observed by fluorescence microscopy. B. Relative expression of several important proteins in the cell cycle and apoptosis were analyzed by western blotting. PI, propidium iodide; H, Hoechst 33342; M, merge. Results display the mean \pm SEM from triplicate experiments. *P < 0.05, compared with NC-sgRNA.

of cells in G0/G1 phase and decreased that in S and G2/M phase in comparison with the negative control. Moreover, to knockdown NUDCD1 significantly increased the percentage of apoptotic cells compared to the negative control (Figures 6, 7A). To explore the molecular mechanism of how NUDCD1 regulated cell cycle and apoptosis, we analyzed the expressions of several important proteins in the cell cycle arrest and apoptosis, cyclin D1, Bcl2, and caspase3, by western blotting. Our results demonstrated that to knockdown NUDCD1 decreased the expression of cyclin D1 and Bcl2, increased the expression of cleaved-caspase3 (Figure 7B).

To knockdown NUDCD1 inhibited the IGF1R-ERK1/2 signaling pathway in vitro and in vivo

Over-expression of NUDCD1 enhanced the proliferation, invasion, and survival of HO-8910 cells via IGF-1R-MAPK signaling pathway [10]. However, NUDCD1's effects on the IGF-1R-MAPK signaling pathway in CRC in vitro and in vivo remain unclear. Therefore, we investigated its effects on this signaling pathway in CRC. IGF-1R inhibitor, linsitinib (50 nM), was set as a positive control *in vitro*. As shown in Figure 8, NUDCD1 knockdown significantly decreased the phosphorylation of phospho-IGF1R (P-IGF1R) and phospho-ERK1/2 (P-ERK1/2) in HCT-116 and HT29 cells, suggesting that NUDCD1 knockdown significantly inhibited IGF-1R-MAPK signaling pathway in CRC in vitro. Likewise, to knockdown NUDCD1 in vivo could significantly suppress the CRC carcinogenesis and metastasis in nude mice (Figure 9A-C), paralleling with the reduced phosphorylation of P-IGF1R and P-ERK1/2 (Figure 9D). Our results indicated that NUDCD1 promotes the malignancy and metastasis

of CRC through regulating IGF1R-ERK1/2 signaling pathway.

Discussion

NUDCD1 (OVA66) is precisely identical to the CML66 which was initially identified in a chronic myelogenous leukemia (CML) cDNA expression library [17]. NUDCD1t promoted the proliferation, invasion, and survival of HeLa cells as an oncoprotein [18]. To explore the effects of NUDCD1 in CRC, we investigated the expressions of NUDCD1 in CRC tissues and cell lines. NUDCD1 was demonstrated to be up-regulated in CRC tissues compared to pericarcinous tis-

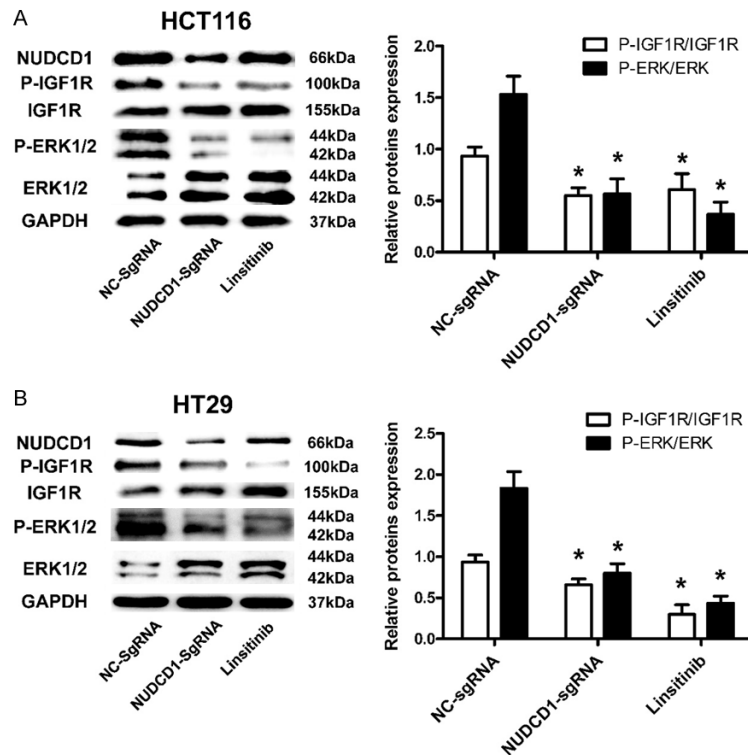


Figure 8. To knockdown NUDCD1 inactivated IGF1R-ERK1/2 signaling pathway in vitro. Relative proteins expression of P-IGF1R and P-ERK1/2 in HCT116 (A) and HT29 cells (B). Results display the mean \pm SEM from triplicate experiments. *P < 0.05, compared with NC-sgRNA.

sues. The expression of NUDCD1 was higher in all of the five CRC cell lines compared to NCM460 cells. To knockdown NUDCD1 resulted in decreased proliferation, invasion and metastasis of CRC cells. Collectively, our data demonstrated that NUDCD1 was over-expressed in CRC tissues and cell lines.

Recent studies reported a series of biological effects of NUDCD1 in tumor cells, not only about immune responses [19-22] but also about apoptosis or other functions [10, 11]. To verify our hypothesis about NUDCD1 in CRC, we analyzed the correlation of NUDCD1 expression with pathological characteristics of 70 CRC patients. To our knowledge, it is the first study which demonstrated that NUDCD1 promotes metastasis in human CRC. We demonstrated that NUDCD1 expression was lower in surrounding pericarcinoma tissues compared to CRC tissues, increased in early stage tumor tissues, and reached the highest level in advanced stage invasive tumor tissues. The expression levels of NUDCD1 were also correlated with poor clinical features including lymph

node metastasis, distant metastasis, and advanced stages. This progressively increased expression profile was paralleled with the disease deterioration, suggesting an oncogenic role of NUDCD1 in CRC. However, further in vitro study was needed to elucidate the mechanism of NUDCD1.

CRISPR/Cas9 plasmids of NUDCD1, NUDCD1-sgRNA, and its corresponding negative control, NC-sgRNA, were chemically synthesized to knockdown NUDCD1 in HCT116 and HT29 cells. We demonstrated that to knockdown NUDCD1 significantly decreased the proliferation of HCT116 and HT29 cells. Down-regulation of NUDCD1 led to a severe reduction of cells which passed through the transwell chamber membrane in the way of migration and invasion. Moreover, we found that to knockdown NUDCD1

suppressed the progression of EMT via decreasing the expression of N-cadherin and increasing the expression of E-cadherin [23].

As reported, active cell cycle and apoptosis signaling play a critical role in tumor development [24, 25]. NUDCD1-sgRNA and NC-sgRNA transfected CRC cells were stained with PI. Data showed that there was a cell cycle accumulation in period G0/G1 and a decline of cell percentage in period G2 after transfection of NUDCD1-sgRNA. In addition, CRC cells were stained with Annexin V-FITC/PI and Hoechst/PI, then analyzed by Flow cytometer and fluorescence microscope. We observed that NUDCD1 could inhibit the apoptosis of CRC cells, just as its role in NIH3T3 and other cancer cells [10, 11]. We also determined the expressions of cyclin D1, Bcl2, caspase3, and cleaved-caspase3 [26-28]. Our results showed that to knockdown NUDCD1 decreased the protein expression of cyclin D1, Bcl2 and increased the protein expression of cleaved-caspase3 in HCT116 and HT29 cell lines. These results

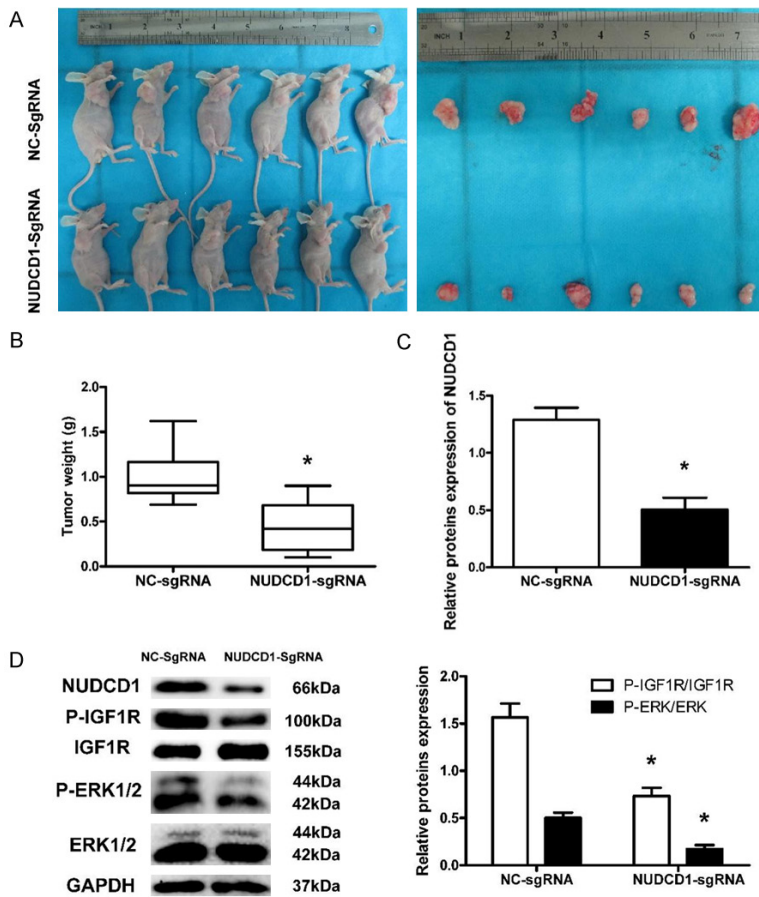


Figure 9. To knockdown NUDCD1 inactivated IGF1R-ERK1/2 signaling pathway in vivo. Volume (A) and weight (B) of subcutaneously xenografted CRC in nude mice. (C) Relative expression of NUDCD1 in xenografted CRC tissues. (D) Relative protein expression of P-IGF1R and P-ERK1/2 in xenografted CRC tissues. Results display the mean \pm SEM from triplicate experiments. *P < 0.05, compared with NC-sgRNA.

indicated the critical roles of NUDCD1 in regulating tumor cell cycle and apoptosis in CRC.

Down-regulation of NUDCD1 had been reported to inhibit the IGF1R-ERK1/2 signaling pathway in cervical and ovarian cancer cells [10]. The hyper-activation of ERK1/2 signaling pathway can promote the malignant biological behavior of CRC cells [29, 30], while the inhibition of ERK1/2 signaling pathway can affect the expressions of the proteins related to proliferation, metastasis, invasion, cycle, and apoptosis [31-35]. In our study, NUDCD1 knockdown significantly inhibited the phosphorylation of P-IGF1R and P-ERK1/2 of CRC cells in vitro and in vivo, indicating that NUDCD1 can inhibit the IGF-1R-MAPK signaling pathway in CRC. Changes in IGF1R signaling theoretically result in changes of p-Akt. But the expression of p-Akt

and total Akt did not change after knocking down NUDCD1 in our preliminary study (data not shown). So NUDCD1 may inhibit the changes of p-Akt through other mechanisms in CRC cells.

In conclusion, we demonstrated that NUDCD1 can promote carcinogenesis and metastasis of CRC through inducing EMT and inhibiting apoptosis, which suggested that NUDCD1 may serve as a biomarker or a target for metastasis of CRC patients.

Acknowledgements

The authors would like to thank Sichuan University for the support in this study. This work was supported by the Fund of Health and Family Planning Commission, Sichuan Province (grant number: 16PJ136).

Disclosure of conflict of interest

None.

Address correspondence to: Yin Liu and Li-Ming Zhou, Department of Pharmacology, West China School of Preclinical and Forensic Medicine, Sichuan University, Chengdu 610041, Sichuan Province, China. Tel: +86 028 85503767; E-mail: yin.liu@scu.edu.cn (YL); zhoulm108@163.com (LMZ)

References

- [1] Jemal A, Bray F, Center MM, Ferlay J, Ward E and Forman D. Global cancer statistics. *CA Cancer J Clin* 2011; 61: 69-90.
- [2] Dent OF, Newland RC, Chan C, Bokey L and Chapuis PH. Trends in pathology and long-term outcomes after resection of colorectal cancer: 1971-2013. *ANZ J Surg* 2017; 87: 34-38.
- [3] Lee HJ, Ye BD, Byeon JS, Kim J, Park YS, Hong YS, Yoon YS and Yang DH. Unusual local recurrence with distant metastasis after successful endoscopic submucosal dissection for colorectal mucosal cancer. *Clin Endosc* 2017; 50: 91-95.

- [4] Chen W, Zheng R, Baade PD, Zhang S, Zeng H, Bray F, Jemal A, Yu XQ and He J. Cancer statistics in China, 2015. *CA Cancer J Clin* 2016; 66: 115-132.
- [5] Cai SD, Chen JS, Xi ZW, Zhang LJ, Niu ML and Gao ZY. MicroRNA144 inhibits migration and proliferation in rectal cancer by downregulating ROCK1. *Mol Med Rep* 2015; 12: 7396-7402.
- [6] Dow LE, O'Rourke KP, Simon J, Tschaharganeh DF, van Es JH, Clevers H and Lowe SW. Apc restoration promotes cellular differentiation and reestablishes crypt homeostasis in colorectal cancer. *Cell* 2015; 161: 1539-1552.
- [7] Wang J, Huang F, Bai Z, Chi B, Wu J and Chen X. Curcumol inhibits growth and induces apoptosis of colorectal cancer LoVo cell line via IGF-1R and p38 MAPK pathway. *Int J Mol Sci* 2015; 16: 19851-19867.
- [8] Yan Y, Phan L, Yang F, Talpaz M, Yang Y, Xiong Z, Ng B, Timchenko NA, Wu CJ, Ritz J, Wang H and Yang XF. A novel mechanism of alternative promoter and splicing regulates the epitope generation of tumor antigen CML66-L. *J Immunol* 2004; 172: 651-660.
- [9] Yang XF, Wu CJ, McLaughlin S, Chillemi A, Wang KS, Canning C, Alyea EP, Kantoff P, Soiffer RJ, Dranoff G and Ritz J. CML66, a broadly immunogenic tumor antigen, elicits a humoral immune response associated with remission of chronic myelogenous leukemia. *Proc Natl Acad Sci U S A* 2001; 98: 7492-7497.
- [10] Rao W, Li H, Song F, Zhang R, Yin Q, Wang Y, Xi Y and Ge H. OVA66 increases cell growth, invasion and survival via regulation of IGF-1R-MAPK signaling in human cancer cells. *Carcinogenesis* 2014; 35: 1573-1581.
- [11] Rao W, Xie G, Zhang Y, Wang S, Wang Y, Zhang H, Song F, Zhang R, Yin Q, Shen L and Ge H. OVA66, a tumor associated protein, induces oncogenic transformation of NIH3T3 cells. *PLoS One* 2014; 9: e85705.
- [12] Rao X, Huang X, Zhou Z and Lin X. An improvement of the 2⁻(-delta delta CT) method for quantitative real-time polymerase chain reaction data analysis. *Biostat Bioinforma Biomath* 2013; 3: 71-85.
- [13] Joung J, Konermann S, Gootenberg JS, Abudayyeh OO, Platt RJ, Brigham MD, Sanjana NE and Zhang F. Genome-scale CRISPR-Cas9 knockout and transcriptional activation screening. *Nat Protoc* 2017; 12: 828-863.
- [14] Zhang Y, Xiao Q, Zhang H, Sun X, Ge H, Liu X, Guan L and Sun M. Adenomatous polyposis coli determines sensitivity to the EGFR tyrosine kinase inhibitor gefitinib in colorectal cancer cells. *Oncol Rep* 2014; 31: 1811-1817.
- [15] Yang K, Tang XD, Guo W, Xu XL, Ren TT, Ren CM, Wang SD, Bao X, Zhang F and Sun KK. BMPR2-pSMAD1/5 signaling pathway regulates RUNX2 expression and impacts the progression of dedifferentiated chondrosarcoma. *Am J Cancer Res* 2016; 6: 1302-1316.
- [16] Zhou JN, Zeng Q, Wang HY, Zhang B, Li ST, Nan X, Cao N, Fu CJ, Yan XL, Jia YL, Wang JX, Zhao AH, Li ZW, Li YH, Xie XY, Zhang XM, Dong Y, Xu YC, He LJ, Yue W and Pei XT. MicroRNA-125b attenuates epithelial-mesenchymal transitions and targets stem-like liver cancer cells through small mothers against decapentaplegic 2 and 4. *Hepatology* 2015; 62: 801-815.
- [17] Jin S, Wang Y, Zhang Y, Zhang HZ, Wang SJ, Tang JQ, Chen HJ and Ge HL. Humoral immune responses against tumor-associated antigen OVA66 originally defined by serological analysis of recombinant cDNA expression libraries and its potentiality in cellular immunity. *Cancer Sci* 2008; 99: 1670-1678.
- [18] Wang Q, Li M, Wang Y, Zhang Y, Jin S, Xie G, Liu Z, Wang S, Zhang H, Shen L and Ge H. RNA interference targeting CML66, a novel tumor antigen, inhibits proliferation, invasion and metastasis of HeLa cells. *Cancer Lett* 2008; 269: 127-138.
- [19] Suemori K. [Induction and functional analysis of cytotoxic T lymphocytes specific for the novel tumor-associated antigen CML66]. *Rinsho Ketsueki* 2009; 50: 604-610.
- [20] Suemori K, Fujiwara H, Ochi T, Azuma T, Yamanouchi J, Narumi H, Yakushijin Y, Hato T, Hasegawa H and Yasukawa M. Identification of an epitope derived from CML66, a novel tumor-associated antigen expressed broadly in human leukemia, recognized by human leukocyte antigen-A*2402-restricted cytotoxic T lymphocytes. *Cancer Sci* 2008; 99: 1414-1419.
- [21] Suemori K, Fujiwara H, Ochi T, Azuma T, Yamanouchi J, Narumi H, Yakushijin Y, Hato T and Yasukawa M. Identification of a novel epitope derived from CML66 that is recognized by anti-leukaemia cytotoxic T lymphocytes. *Br J Haematol* 2009; 146: 115-118.
- [22] Zhang W, Choi J, Zeng W, Rogers SA, Alyea EP, Rheinwald JG, Canning CM, Brusci V, Sasada T, Reinherz EL, Ritz J, Soiffer RJ and Wu CJ. Graft-versus-leukemia antigen CML66 elicits coordinated B-cell and T-cell immunity after donor lymphocyte infusion. *Clin Cancer Res* 2010; 16: 2729-2739.
- [23] Dia VP and Pangloli P. Epithelial-to-mesenchymal transition in paclitaxel-resistant ovarian cancer cells is downregulated by luteolin. *J Cell Physiol* 2017; 232: 391-401.
- [24] Lee E, Decker AM, Cackowski FC, Kana LA, Yumoto K, Jung Y, Wang J, Buttitta L, Morgan TM and Taichman RS. Growth arrest-specific 6 (GAS6) promotes prostate cancer survival by g1 arrest/s phase delay and inhibition of apoptosis.

Molecular mechanisms of colorectal cancer

- tosis during chemotherapy in bone marrow. *J Cell Biochem* 2016; 117: 2815-2824.
- [25] Parmar MB, Arteaga Ballesteros BE, Fu T, K CR, Montazeri Aliabadi H, Hugh JC, Lobenberg R and Uludag H. Multiple siRNA delivery against cell cycle and anti-apoptosis proteins using lipid-substituted polyethylenimine in triple-negative breast cancer and nonmalignant cells. *J Biomed Mater Res A* 2016; 104: 3031-3044.
- [26] Eyvani H, Moghaddaskho F, Kabuli M, Zekri A, Momeny M, Tavakkoly-Bazzaz J, Alimoghaddam K, Ghavamzadeh A and Ghaffari SH. Arsenic trioxide induces cell cycle arrest and alters DNA methylation patterns of cell cycle regulatory genes in colorectal cancer cells. *Life Sci* 2016; 167: 67-77.
- [27] Abaza MS, Afzal M, Al-Attayah RJ and Guleri R. Methylferulate from *Tamarix aucheriana* inhibits growth and enhances chemosensitivity of human colorectal cancer cells: possible mechanism of action. *BMC Complement Altern Med* 2016; 16: 384.
- [28] Semaan J, Pinon A, Rioux B, Hassan L, Limami Y, Pouget C, Fagnere C, Sol V, Diab-Assaf M, Simon A and Liagre B. Resistance to 3-HTMC-induced apoptosis through activation of PI3K/Akt, MEK/ERK, and p38/COX-2/PGE2 pathways in human HT-29 and HCT116 colorectal cancer cells. *J Cell Biochem* 2016; 117: 2875-2885.
- [29] Liu H, Zhang Q, Li K, Gong Z, Liu Z, Xu Y, Swaney MH, Xiao K and Chen Y. Prognostic significance of USP33 in advanced colorectal cancer patients: new insights into beta-arrestin-dependent ERK signaling. *Oncotarget* 2016; 7: 81223-81240.
- [30] Rey C, Faustin B, Mahouche I, Ruggieri R, Brulard C, Ichas F, Soubeyran I, Lartigue L and De Giorgi F. The MAP3K ZAK, a novel modulator of ERK-dependent migration, is upregulated in colorectal cancer. *Oncogene* 2016; 35: 3190-3200.
- [31] Liu CH, Huang Q, Jin ZY, Zhu CL, Liu Z and Wang C. miR-21 and KLF4 jointly augment epithelial-mesenchymal transition via the Akt/ERK1/2 pathway. *Int J Oncol* 2017; 50: 1109-1115.
- [32] Gorowska-Wojtowicz E, Hejmej A, Kaminska A, Pardyak L, Kotula-Balak M, Dulinska-Litewka J, Laidler P and Bilinska B. Anti-androgen 2-hydroxyflutamide modulates cadherin, catenin and androgen receptor phosphorylation in androgen-sensitive LNCaP and androgen-independent PC3 prostate cancer cell lines acting via PI3K/Akt and MAPK/ERK1/2 pathways. *Toxicol In Vitro* 2017; 40: 324-335.
- [33] Tian Y, Wang J, Wang W, Ding Y, Sun Z, Zhang Q, Wang Y, Xie H, Yan S and Zheng S. Mesenchymal stem cells improve mouse non-heart-beating liver graft survival by inhibiting Kupffer cell apoptosis via TLR4-ERK1/2-Fas/FasL-caspase3 pathway regulation. *Stem Cell Res Ther* 2016; 7: 157.
- [34] Bai T, Liu F, Zou F, Zhao G, Jiang Y, Liu L, Shi J, Hao D, Zhang Q, Zheng T, Zhang Y, Liu M, Li S, Qi L and Liu JY. Epidermal growth factor induces proliferation of hair follicle-derived mesenchymal stem cells through epidermal growth factor receptor-mediated activation of ERK and AKT signaling pathways associated with upregulation of cyclin D1 and downregulation of p16. *Stem Cells Dev* 2017; 26: 113-122.
- [35] Chen J, Chen J, Wang X, Wang C, Cao W, Zhao Y, Zhang B, Cui M, Shi Q and Zhang G. Ligustrazine alleviates acute pancreatitis by accelerating acinar cell apoptosis at early phase via the suppression of p38 and Erk MAPK pathways. *Biomed Pharmacother* 2016; 82: 1-7.